ISSN 0006-3509, Biophysics, 2017, Vol. 62, No. 6, pp. 885–891. © Pleiades Publishing, Inc., 2017.
Original Russian Text © A.V. Popinako, M.Yu. Antonov, A.S. Chemeris, K.V. Shaitan, O.S. Sokolova, 2017, published in Biofizika, 2017, Vol. 62, No. 6, pp. 1077–1083.

MOLECULAR BIOPHYSICS

Analysis of the Interactions between Arp2/3 Complex and an Inhibitor Arpin by Molecular Dynamics Simulation

A. V. Popinako[a], M. Yu. Antonov[b], A. S. Chemeris[c], K. V. Shaitan[c, d], and O. S. Sokolova[c, *]

[a] *Bach Institute of Biochemistry, Research Center of Biotechnology, Russian Academy of Sciences, Moscow, 119071 Russia*
[b] *Ammosov Northeastern Federal University, Yakutsk, Republic of Sakha (Yakutia), 677980 Russia*
[c] *Moscow State University, Moscow, 119991 Russia*
[d] *Semenov Institute of Chemical Physics, Russian Academy of Sciences, Moscow, 119991 Russia*
**e-mail: sokolova@mail.bio.msu.ru*

Received June 5, 2017

Abstract—The Arp2/3 complex is one of the main regulators of the actin cytoskeleton and a basic molecular machine that nucleates the branched actin filaments. In this work, we studied the interaction of the Arp2/3 complex with its inhibitor, arpin, and revealed the amino-acid residues that are responsible for complex formation. The free-energy calculation for arpin binding to the Arp2/3 complex was performed using umbrella sampling. It has been shown that the dissociation constant of the Arp2/3–arpin complex is higher on average than that of Arp2/3 complexes with other inhibitors. Two arpin binding sites with different affinities were identified on the surface of the Arp2/3 complex. The mechanism of the inhibition of the Arp2/3 complex by arpin is discussed.

Keywords: Arp2/3 complex, arpin, inhibition, molecular modeling
DOI: 10.1134/S0006350917060203

The ability of cells to migrate is an integral part of such important physiological processes as repair, embryonic development, and the immune response. Disturbances in cell motility lead to the development of pathological processes in the body. Thin membrane protrusions on the leading edge of the cell called lamellipodia, which contain a branched network of actin filaments, are responsible for cell migration.

The Arp2/3 complex is one of the main regulators of the actin cytoskeleton and a basic molecular machine that nucleates branched actin filaments. In the presence of ATP, activators of the Arp2/3 complex, and a pool of actin monomers, the Arp2/3 complex forms a so-called "branch junction" that initiates the growth of a daughter actin filament at an angle of 70° to the maternal filament. The daughter filament contains a barbed end for connection of new actin monomers and further elongation. It is known that in the cytoplasm the Arp2/3 complex naturally fluctuates between open (inactive) and closed (active) conformational states [1]. When the Arp2/3 complex is activated, the Arp2 and Arp3 subunits approach each other; since these subunits are actin-like, they create a platform for attachment of actin monomers in the growing daughter filament. Arp2/3 complex activators such as WASP (the Wiskott–Aldrich syndrome protein) and WAVE (the WASP-family verprolin-homologous protein) have a C-terminal VCA domain consisting of three motifs: V is the verproline-like motif, C is the central (cofilin-like) motif, and A is an acidic motif. The VCA domain is responsible for binding to the Arp2/3 complex and promotes convergence of the Arp2 and Arp3 subunits [2]. Previously, it has been thought that the stoichiometry of interaction of the Arp2/3 complex with an activator is 1 : 1. In 2014, a paper was published in which the authors showed the possibility of interaction of two VCA domains with one Arp2/3 complex using a biochemical approach and Förster resonance energy transfer (FRET) microscopy. The authors also measured the distance between individual motifs of the VCA domain and proposed a molecular model of the Arp2/3 complex in the active conformation [2].

The branching of actin filaments is a complex process; many proteins are involved in its regulation. In addition to positive regulation, the Arp2/3 complex also undergoes negative regulation by such inactivation proteins as GMF (glia maturation factor) [3] and coronin [4], which transfer the Arp2/3 complex to an open (inactive) state [5].

In 2013, arpin was found for the first time in lamellopodia using bioinformatic analysis by homology with Arp2/3 complex activators and an Arp2/3 inactivator [6]. Arpin is a relatively small (25 kDa) protein; it possesses an A motif on its C-terminus, lacking C and V motifs. Using biochemical methods, it has been

(a)

```
sp|Q7Z6K5|ARPIN_HUMAN      ----------------------------------------GDGKTGASWTDNIMAQKC 18
sp|P42768|WASP_HUMAN       PAGGLAPGGGRGALLDQIRQGIQLNKTPGAPESSALQPPPQSSEGLVGALMHVMQKRSRA 480
                                                                  .:* .**        .:.

sp|Q7Z6K5|ARPIN_HUMAN      SKGAAAEIREQGDGAEDEEWDD 40
sp|P42768|WASP_HUMAN       IHSSDEGEDQAGDEDEDDEWDD 502
                            . .     . **  **.****
```

(b)

(c)

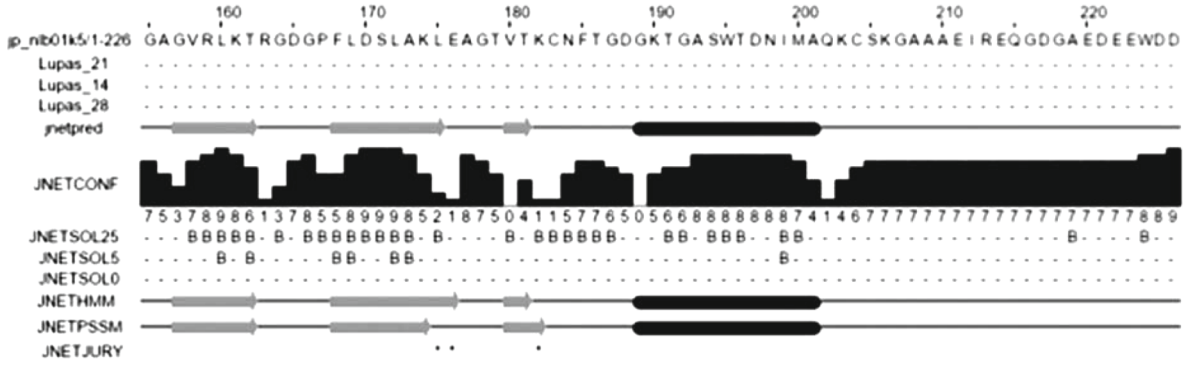

Fig. 1. (a) The alignment of the arpin amino-acid sequences; (b) a model of the C-terminal fragment of arpin (the GDGKTGAS-WTDN spiral is highlighted by a contour); (c) prediction of the secondary structure of arpin in the JPred program [13].

shown that arpin overexpression leads to a decrease in the number of branched acting filaments, while when arpin is suppressed the motile cells move more directly. In 2016, a structural model of arpin based on SAXS-analysis scattering data was published (PDB ID 4Z68) [7]. According to this model, the C-terminus of arpin is mobile and unstructured; the authors also showed that one arpin binding site to the Arp2/3 complex is located between the Arp2 and ARPC1 subunits of the Arp2/3 complex [7]. We previously determined a second binding site to arpin that is located on the Arp3 subunit of the Arp2/3 complex using single particle EM [5, 8].

The aim of this study was to investigate the interaction of arpin with the Arp2/3 complex and to identify the amino-acid residues involved in their binding at two sites. For this, we used methods of molecular modeling.

METHODS

Modeling the interaction of arpin with the Arp2/3 complex in two binding sites. The procedure for searching for structural patterns of the C-terminal fragment of arpin (UniProtID: Q7Z6K5) was performed using BLAST [9]. As a result, the 4Z68_E [7] and 1T84_A [10] structures (the EIREQGDGAEDE sequence) were selected as templates for building the model. The alignment of the amino-acid sequences of arpin and the VCA domain (WASP protein) was performed "using the" T-COFFEE software [11] (Fig. 1a). Based on this alignment, a model of the arpin structure (Fig. 1b) was constructed using the MODELLER software [12]. The models were ranked according to the values of the moldpdf and DOPE scores [12]; as a result, the optimal model with a high rating was chosen. The result of modeling the secondary structure of arpin coincided with the location of the GDGKTGAS-WTDN spiral predicted in the JPred software [13].

The calculated arpin model was docked in two binding sites that we identified previously by transmission electron microscopy [5] using the HADDOCK [14] and UCSF Chimera programs and taking the predicted location of the VCA domain of the Arp2/3 complex activators into account [15] (Fig. 2).

Molecular dynamics. To study the interaction of the Arp2/3 complex with inhibitor, we calculated and analyzed the molecular-dynamics trajectories of the

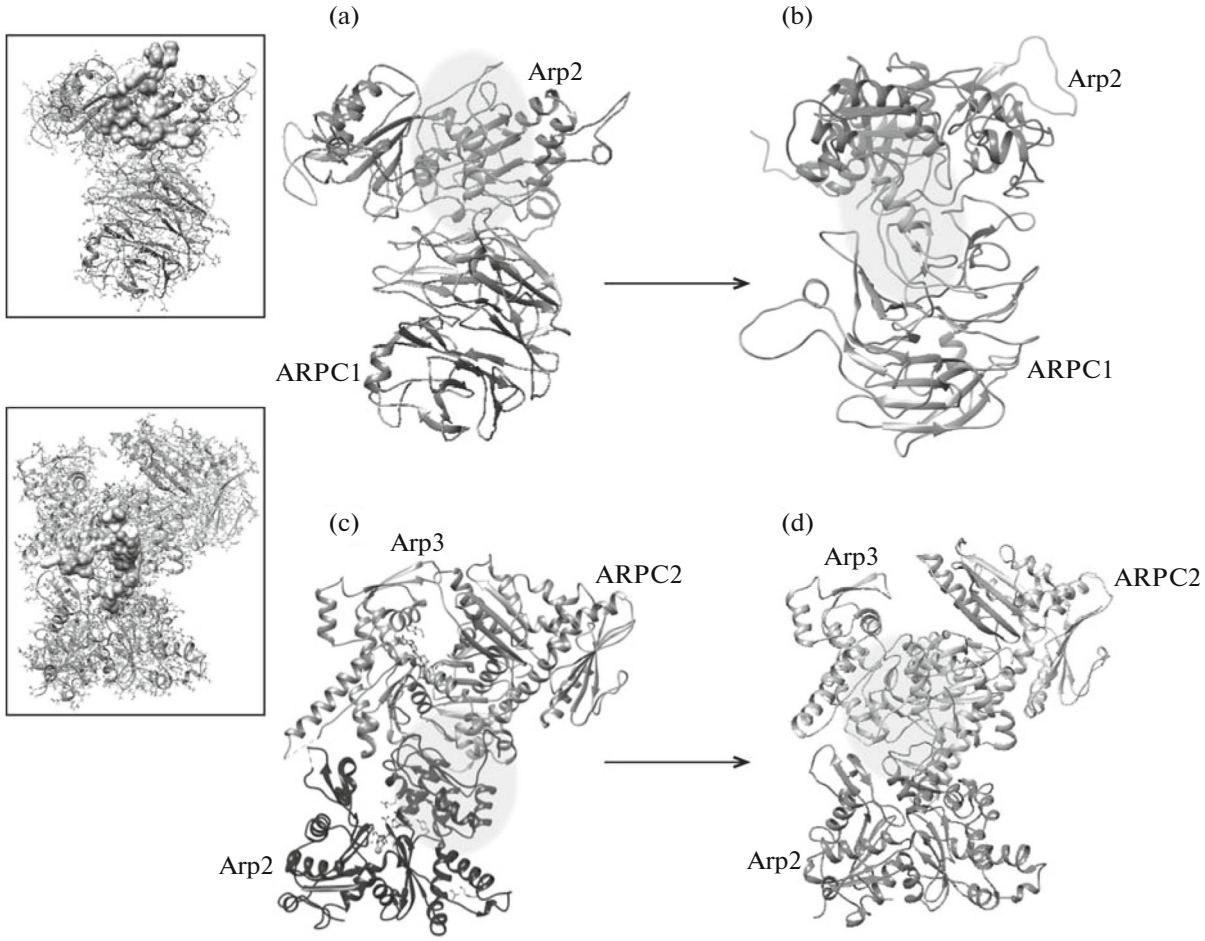

Fig. 2. Simulation of interactions in the Arp2/3–arpin complex. Subunits of the Arp2/3 complex are designated; arpin is highlighted by gray circles. (a) A model of arpin in the ARPC1 site of the Arp2/3 complex before molecular dynamics; (c) a model of arpin in the Arp3 site of the Arp2/3 complex before molecular dynamics; (b), (d) the results of calculation in the HADDOCK program, respectively.

arpin complex in two binding sites (full-atom models of the Arp2/3 complex with arpin in two binding sites were used for calculations). The first system consisted of Arp2, ARPC1 subunits, arpin, ions, and aqueous environment (SPC216 water model). The second system consisted of Arp2, Arp3, ARPC2 subunits, arpin, ions, and the aqueous environment (SPC216 water model).

We used the Gromacs 4 software package [16] and the OPLS-AA force field [17] for calculations. Rectangular computational boxes were used for calculations. The box size was selected in such a way that the smallest distance from the protein to box boundary was not less than 1 nm. The calculated trajectory length was 15 ns (1 ns for relaxation), the integration step was 1 fs. The calculations were carried out in a periodic box using a Berendsen thermostat (a maintained temperature 300 K). The cutoff radius $R_{VdW} = 18$ Å was used to take the van-der-Waals and Coulomb interactions into account. All calculations were carried out using the computing resources of the supercomputer complex of the Moscow State University [18] and the Arian Kuzmin supercomputer of the Ammosov Northeastern Federal University (Yakutsk, Russia). The UCSF Chimera software was used for visualization [19]. Different types of contacts in molecules were calculated using the Protein Interactions Calculator (PIC) server [20].

Calculation of the free binding energy. To calculate the free energy of arpin binding to the Arp2/3 complex, we selected a model of the Arp2/3 complex and arpin in the Arp3 binding site: the Arp2 and ARPC1 subunits that interact with arpin were isolated. The complex was placed in a cell with dimensions of 22.1 × 11.6 × 10.1 nm and the box was filled with water (the SPC216 water model). The electroneutrality of the solution was achieved by the addition of anti-ions. The molecular-dynamics calculation of the system was carried out under isobaric–isothermal conditions; the temperature was maintained at 300 K; the pressure remained constant and equal to 1 bar. The GROMOS 53a6 force field was used for calculations. The trajec-

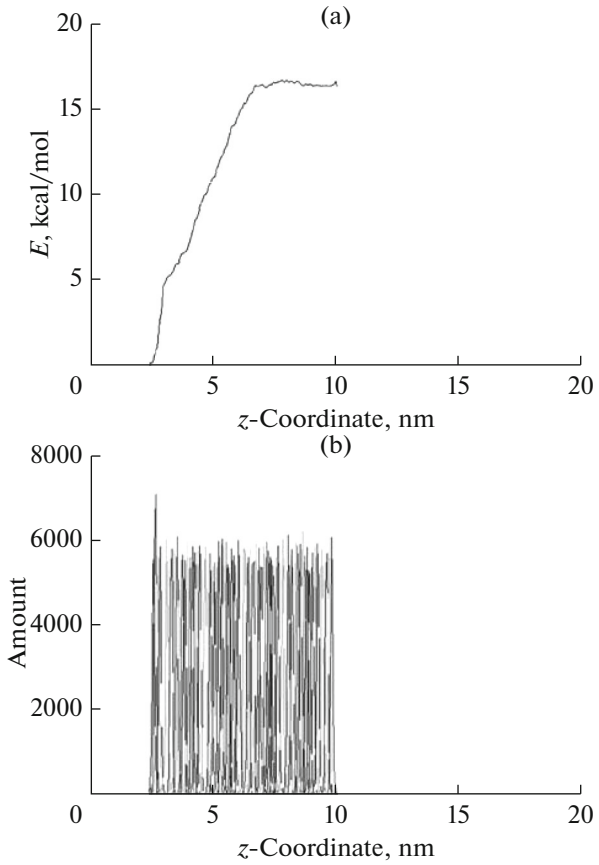

Fig. 3. The results of the calculation of the free binding energy in the Arp2/3–arpin complex: (a) the dependence of the potential of mean force on the distance between the centers of masses of arpin in the ARPC1 site and the Arp2/3 complex; (b) a histogram of sample configurations for the calculation of the results of umbrella sampling by the weighted analysis of histograms.

tory corresponding to the removal of arpin from the Arp2/3 complex by 4 nm (along the reaction coordinate) determined the starting configurations necessary for calculating the potential of the mean force (total, 73 configurations). No interactions between arpin and Arp2/3 complex were detected after 800 pc at the distances of ~4 nm (812 frames) and further, since in this fragment of the trajectory, the distance between the centers of masses of arpin and the Arp2/3 complex changes directly in proportion to time. We then performed a molecular-dynamics calculation for each point of the arpin conformational space relative to the Arp2/3 complex (73 calculations) along the reaction coordinate. The trajectory lengths were 10 ns, the total calculation time of the molecular-dynamics trajectories was 2 μs. Calculation of the potential of mean force and binding energy was carried out using the method of weighted analysis of histograms (Fig. 3). The histograms of sample configurations for umbrella sampling calculations show the overlap between neighboring configurations more than 5 nm. Thus, this method allows one to obtain reliable results.

RESULTS AND DISCUSSION

In this paper, the study of the Arp2/3 complex inactivation by computer simulation methods was based on previously published structural data on the protein–protein interactions in the complex of the Arp3 subunit and the C-terminal fragment of the VCA domain (X-ray diffraction data) [21], on the interactions in the complex of the ARPC1 subunit and the C-terminal fragment of the VCA domain (nuclear magnetic resonance spectroscopy data) [22], and on the three-dimensional structure of the open (inhibited) Arp2/3 complex with two arpins (transmission electron microscopy data) [5].

We used the homology-modeling method to build the models. A molecular model of the Arp2/3 complex interacting with arpin was constructed according to previously obtained transmission electron microscopy data that showed that arpin, like the VCA domains of activators, has two binding sites on the Arp2/3 complex [5]. The identified sites are located between the ARPC1 and Arp2 subunits of the complex (hereinafter designated as the ARPC1 site) and between the Arp3 and ARPC3 subunits (hereinafter designated as the Arp3 site).

Analysis of the interaction of the Arp2/3 complex with arpin in the ARPC1 site. Analysis of the contact surface of the Arp2/3 complex and arpin (the contact surface area between the Arp2/3 complex and arpin was ~1000 Å^2) in the hydrophobic–hydrophilic representation revealed the presence of a hydrophobic interface between arpin and the Arp2 subunit formed by Trp38(arpin) and Tyr222, Tyr225(Arp2) (Fig. 2a).

Hydrophobic interactions occur, along with hydrogen bonds and salt bridges between arpin and the Arp2/3 complex: (Asp2(arpin)–Lys339(Arp2), Glu25(arpin)–Lys138(ARPC1), Asp31(arpin)–Lys322, Arg343, Lys341(Arp2), Glu34(arpin)–Arg343(Arp2), Arg94(ARPC1), Asp35(Arp2)–His51(ARPC1), Asp35(arpin)–Arg94(ARPC1), and Glu37(arpin)–Arg94(ARPC1)).

Analysis of the molecular-dynamics trajectory of the Arp2/3 complex and arpin in the ARPC1 site revealed the occurrence of new hydrophobic–hydrophobic interactions (Fig. 4a): Ala23(arpin)–Val119(ARPC1) and the Asp31(arpin)–Arg74(ARPC1), Glu34(arpin)–His51(ARPC1), Asp31(arpin)–Arg94(ARPC1), Glu34(arpin)–Arg94(ARPC1), Glu37(arpin)–Arg74(ARPC1), Glu37(arpin)–Arg343(Arp2), and Asp40(arpin)–Lys322(Arp2) hydrogen bonds. The Glu25(arpin)–Lys138(ARPC1) bond proved to be the strongest. The Lys138 residue in the ARPC1 subunit and the residues that are closest to it form a positively charged surface of Lys135–His136–Lys138–Lys139 (a 'lysine motif').

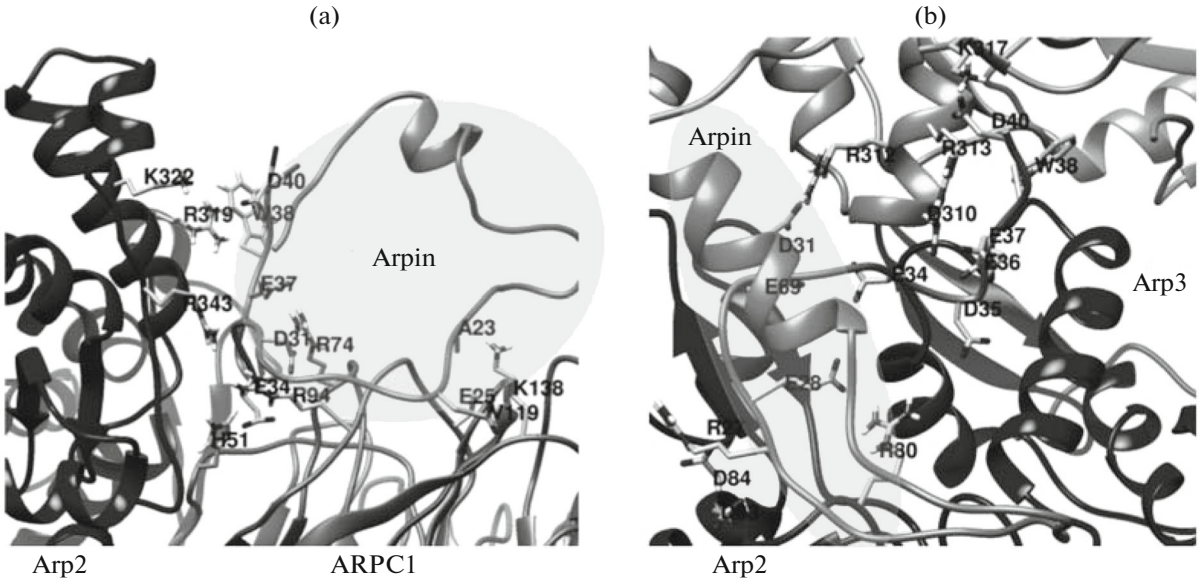

Fig. 4. Arpin binding sites: left, ARPC1-site; right, Arp3-site. Subunits are indicated.

This motif can be a target for binding of negatively charged domains (it is known that arpin is negatively charged). Such lysine motifs are widely distributed in nature and play an important role in protein signaling: attraction of positively charged ions and protein–protein interactions [23–26].

Analysis of the interaction of the Arp2/3 complex with arpin in the Arp3 site. The contact surface area between the Arp2/3 complex and arpin in the Arp3 site is ~528 Å^2 between arpin and the Arp3 subunit, and 490 Å^2 between arpin and the Arp2 subunit. Analysis of the contact surface of the Arp2/3 complex and arpin in the hydrophobic–hydrophilic representation revealed the presence of a hydrophobic interface formed by the following amino-acid residues: Ala23Trp38(arpin), Ile78(Arp3), and Pro314(Arp2).

Hydrogen bonds also occur along with these hydrophobic interactions. The atomic model of the Arp2/3 complex with arpin in the Arp3 site obtained by docking (Fig. 2c) is formed by six hydrogen bonds between arpin and the Arp3 subunit and eight hydrogen bonds between arpin and the Arp2 subunit, as well as by salt bridges: Arg27(arpin)–Asp83(Arp3), Arg27(arpin)–Asp84(Arp3), Glu28(arpin)–Arg80(Arp3), Glu28(arpin)–Asp84(Arp3), Asp31(arpin)–Arg312(Arp2), Asp31(arpin)–Glu69(Arp3), Glu34(arpin)–Arg312(Arp2), Glu34(arpin)–Asp310(Arp2), Asp35(arpin)–Asp310(Arp3), Asp35(arpin)–Arg80(Arp2), Glu36(arpin)–Asp310(Arp3), Glu37(arpin)–Asp310(Arp3), Glu37(arpin)–Arg313(Arp2), Asp40(arpin)–Arg313(Arp3), and Asp40(arpin)–Lys317(Arp3).

Analysis of the molecular-dynamics trajectories of the Arp2/3 complex in the Arp3 site revealed the occurrence of a new hydrophobic contact between Trp38(arpin) and Val311(Arp3). The number of hydrogen bonds between the Arp2/3 complex and arpin also increased. New hydrogen bonds were formed between Glu34(arpin) and Arg80(Arp2). New hydrogen bonds between the Arp3 subunit and arpin occurred: Asp39(arpin)–Lys317(Arp3) and Asp31(arpin)–Arg317(Arp3) (Figs. 2d and 4b).

Estimation of the free energy. The calculation of the free energy of arpin binding to the Arp2/3 complex was performed by umbrella sampling [27]. This method allows one to calculate the free energy based on the values of the potential of the mean force. The potential of the mean force was calculated for a series of conformations obtained as a result of molecular dynamics (Fig. 3).

The free energy (ΔG) of the interaction of arpin and other activators/inhibitors of the Arp2/3 complex was evaluated using the PRODIGY program [28] at 36°C (Table 1). Binding between arpin and the Arp2/3 complex was very strong. The calculated constants of the arpin A domain binding to Arp2/3 were 8–43 times higher than the binding constant of the VCA domain (0.88 μM [22]). The dissociation constant of the Arp2/3–arpin complex was on average higher than that of Arp2/3 complexes with other inhibitors. Interestingly, the dissociation constant of the Arp2/3–arpin complex with arpin in the Arp3 site was significantly higher than with arpin in the ARPC1 site.

Thus, the two arpin binding sites differ in their dissociation constants, which supports the hypothesis of a low-affinity binding site existence in addition to the

Table 1. The free binding energy in the Arp2/3 complex with ligands

Arp2/3–GMF		Arp2/3–VCA	Arp2/3–arpin	
ARPC1 binding site	Arp3 binding site	ARPC1 binding site [5]	ARPC1 binding site	Arp3 binding site
$\Delta G = -5.8$ kcal/mol	$\Delta G = -5.4$ kcal/mol		$\Delta G = -7.3$ kcal/mol	$\Delta G = -10.5$ kcal/mol
$K_d = 5.8$ μM	$K_d = 1.1$ μM	$K_d = 0.88$ μM	$K_d = 6.1$ μM	$K_d = 3.3$ μM

high-affinity site [5]. Stronger binding of arpin than the VCA domain explains the previously suggested mechanism of inhibition of the Arp2/3 complex, which is based on a competitive displacement of the activator's VCA domain from its binding site. Strong binding to the Arp2/3 complex allows arpin to effectively inhibit the branching and growth of a daughter actin filament.

In conclusion, the strength of the interaction between the Arp2/3 complex and arpin in two sites is determined by the presence and number of hydrophobic contacts and hydrogen bonds. In the ARPC1 site, binding occurs due to the formation of hydrophobic contacts and several hydrogen bonds. The hydrogen bonds that form a network of interactions are of great importance in the interaction of the Arp2/3 complex with arpin in the Arp3 site.

ACKNOWLEDGMENTS

Molecular-dynamics calculations and calculation of the free energy of interaction of the Arp2/3 complex with arpin were financially supported by the Russian Science Foundation (project no. 14-14-00234). Simulation of the interaction of arpin with the Arp2/3 complex in two binding sites was financially supported by the Russian Foundation for Basic Research (project no. 16-34-60252). Calculations were carried out using the computing resources of the supercomputer complex of Moscow State University and the Arian Kuzmin supercomputer of the Ammosov Northeastern Federal University (Yakutsk, Russia).

REFERENCES

1. A. A. Rodal, O. Sokolova, D. B. Robins, et al., Nat. Struct. Mol. Biol. **12**, 26 (2005). doi 10.1038/nsmb870
2. R. Gorelik, I. Dang, and A. Gautreau, Med. Sci. (Paris) **30** (3), 248 (2014). doi 10.1051/medsci/20143003010
3. C. A. Ydenberg, S. B. Padrick, M. O. Sweeney, et al., Curr. Biol. **23**, 1037 (2013). doi 10.1016/j.cub.2013.04.058
4. M. Gandhi and B. L. Goode, Subcell. Biochem. **48**, 72 (2008). doi 10.1007/978-0-387-09595-0_7
5. O. S. Sokolova, A. Chemeris, S. Guo, et al., J. Mol. Biol. **429**, 237 (2017). doi 10.1016/j.jmb.2016.11.030
6. I. Dang, R. Gorelik, C. Sousa-Blin, et al., Nature **503**, 281 (2013). doi 10.1038/nature12611
7. S. Fetics, A. Thureau, V. Campanacci, et al., Structure **24**, 252 (2016). doi 10.1016/j.str.2015.12.001
8. S. B. Padrick, L. K. Doolittle, C. A. Brautigam, et al., Proc. Natl. Acad. Sci. U. S. A. **108**, E472 (2011). doi 10.1073/pnas.1100236108
9. S. F. Altschul, W. Gish, W. Miller, et al., J. Mol. Biol. **215**, 403 (1990). doi 10.1016/S0022-2836(05)80360-2
10. J. R. Peterson, L. C. Bickford, D. Morgan, et al., Nat. Struct. Mol. Biol. **11**, 747 (2004). doi 10.1038/nsmb796
11. C. Notredame, D. G. Higgins, and J. Heringa, J. Mol. Biol. **302**, 205 (2000). doi 10.1006/jmbi.2000.4042
12. A. Fiser and A. Sali, Methods Enzymol. **374**, 461 (2003). doi 10.1016/S0076-6879(03)74020-8
13. A. Drozdetskiy, C. Cole, J. Procter, and G. J. Barton, Nucleic Acids Res. **43**, W389 (2015). doi 10.1093/nar/gkv332
14. D. Spiliotopoulos, P. L. Kastritis, A. S. J. Melquiond, et al., Front. Mol. Biosci. **3**, 46 (2016). doi 10.3389/fmolb.2016.00046
15. M. Boczkowska, G. Rebowski, D. J. Kast, and R. Dominguez, Nat. Commun. **5**, 3308 (2014). doi 10.1038/ncomms4308
16. S. Pronk, Sz. Páll, R. Schulz, et al., Bioinformatics **29**, 845 (2013). doi 10.1093/bioinformatics/btt055
17. G. A. Kaminski, J. Phys. Chem. B **109**, 5884 (2005). doi 10.1021/jp050156
18. V. Sadovnichy, A. Tikhonravov, V. Voevodin, and V. Opanasenko, in *Contemporary High Performance Computing: From Petascale toward Exascale* (Chapman & Hall/CRC Press, Boca Raton, USA, 2013), pp. 283–307.
19. E. F. Pettersen, T. D. Goddard, C. C. Huang, et al., J. Comput. Chem. **25**, 1605 (2004). doi 10.1002/jcc.20084
20. K. G. Tina, R. Bhadra, and N. Srinivasan, Nucleic Acids Res. **35**, 473 (2007). doi 10.1093/nar/gkm423
21. S.-C. Ti, C. T. Jurgenson, B. J. Nolen, and T. D. Pollard, Proc. Natl. Acad. Sci. U. S. A. **108**, E463 (2011). doi 10.1073/pnas.1100125108

22. A. E. Kelly, H. Kranitz, V. Dɯtsch, and R. D. Mullins, J. Biol. Chem. **281**, 10589 (2006). doi 10.1074/jbc.M507470200

23. V. O. Kravchuk, O. V. Savytskyi, K. O. Odynets, et al., J. Biomol. Struct. Dyn. **35**, 2759 (2017). doi 10.1080/07391102.2016.1235512

24. A. V. Popinako, T. V. Tikhonova, M. Yu. Antonov, et al., Biophysics (Moscow) **62**, 214 (2017).

25. A. Grizel, A. Popinako, M. A. Kasimova, et al., J. Neuroimmune Pharmacol. **9**, 727 (2014). doi 10.1007/s11481-014-9565-x

26. A.-Q. Sun, Y. Luo, D. S. Backos, et al., Mol. Pharmacol. **83**, 1078 (2013). doi 10.1124/mol.113.084772

27. R. Friedman, E. Nachliel, and M. Gutman, Biophys. J. **89**, 768 (2005). doi 10.1529/biophysj.105.058917

28. L. C. Xue, J. P. Rodrigues, P. L. Kastritis, et al., Bioinformatics, btw514 (2016). doi 10.1093/bioinformatics/btw514

Translated by G. Levit